Journal of
Fisheries and Aquatic Science

ISSN 1816-4927

Academic
Journals Inc.

www.academicjournals.com

Journal of Fisheries and Aquatic Science 8 (5): 581-594, 2013
ISSN 1816-4927 / DOI: 10.3923/jfas.2013.581.594

Spatial and Temporal Variations of Coastal Fishing Area by Satellite Imagery Classification

[1]M.N. Sumardi, [1]A.M. Mustapha, [1]T. Lihan and [2]F. Tangang

[1]School of Environmental and Natural Resource Sciences, Faculty of Science and Technology, Universiti Kebangsaan Malaysia, 43600 Bangi, Selangor, Malaysia

[2]Research Centre for Tropical Climate Change System (IKLIM), School of Environmental and Natural Resource Sciences, Faculty of Science and Technology, Universiti Kebangsaan Malaysia, 43600 Bangi, Selangor, Malaysia

Corresponding Author: A.M. Mustapha, School of Environmental and Natural Resource Sciences, Faculty of Science and Technology, Universiti Kebangsaan Malaysia, 43600 Bangi, Selangor, Malaysia

ABSTRACT

The east coast of Malaysian waters is of importance because it harbors the country's fisheries resources. Determination of its spatial and temporal variations enables understanding of the coastal waters dynamics and physical processes affecting the region. Aqua MODIS satellite data of normalized water-leaving radiance (nLw at 412, 443 and 551 nm) from January 2006 to December 2010 were processed to determine variability using the classification approach. Five spectrally defined classes were obtained to represent the coastal water characteristics based on false color images. Variability was influenced by the outflow of terrestrial water which carries the load of suspended materials into the ocean and it moved according to the northeast and southwest wind and current propagation. Empirical Orthogonal Function (EOF) analysis of nLw 551 imagery explained the variability in temporal and spatial scale. The first mode of the EOF analysis (77.38% of variance) indicated the seasonal cycle. The second mode (4.96% of variance) explained the inter-monsoon period indicating the variability between the two periods of the Northeast and Southwest monsoon in this area. The third mode (3.17% of variance) indicated the Northeast monsoon which showed high variability toward the coastal water region associated with strong wind. The fourth mode (1.91% of variance) explained the Southwest monsoon associated with weakened wind and showed spreading surface pattern further from the coastline. Understanding of this variability would greatly contribute to coastal fisheries management and planning that could provide benefits to the coastal area as well as the productivity of this region.

Key words: Classification, coastal fishing waters, satellite imagery, empirical orthogonal function, wind

INTRODUCTION

Coastal water encompasses many water characteristics and dynamically changes due to natural processes as well as human use. Understanding the physical processes influencing this area is important to enable the implementation of alternative approaches in sustainable management of resources within this area. This area has different structure and size of sediment as well as suspended matter composition. This composition may include large amounts of nutrients, organics,

heavy metals and colored dissolved organic materials (Li *et al*., 2010; Tiwari and Shanmugam, 2011). The change in the composition of suspended materials affects the water column and benthic processes. Many of these compositions are discharged to the coastal region as dissolved and particulate nutrients from land as a result of human activities. Due to the variability of the physical dynamics and seasonal conditions in the coastal region, the biological, chemical and geological attributes will also be affected (Schalles, 2006).

Satellite images are becoming an important method used in monitoring coastal water areas. The radiance of heterogeneous mixtures of suspended and biophysical materials in the water column are reflected and recorded by the Instantaneous-field-of-view (IFOV) of the satellite sensor (Zhang *et al*., 2000). This parameter indicates the variation of hydro-optical properties which are studied over the wavelength range of 400 to 700 nm (Tiwari and Shanmugam, 2011). Determinations are based on the changes in ocean color which focuses on the wavelength of chlorophyll and Colored Dissolved Organic Matter (CDOM) of the spectral normalized water-leaving radiance (nLw) at 412 and 443 nm (Darecki and Stramski, 2004; Nezlin *et al*., 2008; Wang *et al*., 2011; Schroeder *et al*., 2012). Studies of coastal water also suggest that the distribution of suspended matter and turbidity of water column can be observed through the wavelength of 551 nm (Yuan *et al*., 2008). Understanding these variations is important to determine the dynamics of the coastal area. Using ocean color properties, optically determined classified water body will help in understanding the biophysical characteristics of an area. Previous studies have also showed that this method provides qualitative information on the extent and distribution of materials in the coastal area and is utilized in the identification of oceanographic features such as fronts, internal waves, upwelling, gyres, eddies, surface currents, river plume and biological parameters (Sasmal, 1997; Zhang *et al*., 2000; Lihan *et al*., 2008).

The eastern coast of Peninsular Malaysia is strongly influenced by the monsoon period over the South China Sea. During the monsoon period, annual reversal of the winds occurs and is associated with rainy summer and dry winter (Wang *et al*., 2004). According to Kueh and Lin (2010), the transition and onset of these systems happens due to atmospheric internal dynamics, intra-seasonal oscillation and sea/land surface conditions. This factor was observed to be directly related with the East Asian monsoon and the Australian winter monsoon which is affected by the El-Niño Southern Oscillation (ENSO) and other interannual and decadal variations in the Pacific and Indian Ocean (Chang *et al*., 2006). The impact of the El-Niño weather patterns on the monsoon means that the rain zone that is usually centered over the western margin of the Pacific, moves eastward into the central Pacific especially to the Indonesia and Malaysia.

The coast of Pahang (between 2.5°N to 4.5°N and from 103.0°E until 104.45°E) in eastern Peninsular Malaysia (Fig. 1) has an important significance to the coastal environment in the tropical water of South China Sea. Topography of this area is flat and undulating. The main river is the Pahang River (459 km long) which is the longest river in Peninsular Malaysia. The Pahang river system plays an important role in contributing to the transportation and deposition of suspended material and nutrient into the coastal region. River discharge is the main factor that affects coastal water due to the mixture of fine silts, clays and dissolved organic matter (Thomas and Weatherbee, 2006). The coast is also affected by other smaller rivers and several agricultural activities along the coast. Hence, the objectives of this study were to understand the spatial and temporal dynamics of Pahang coastal water and to clarify the seasonal and interannual variability using satellite images.

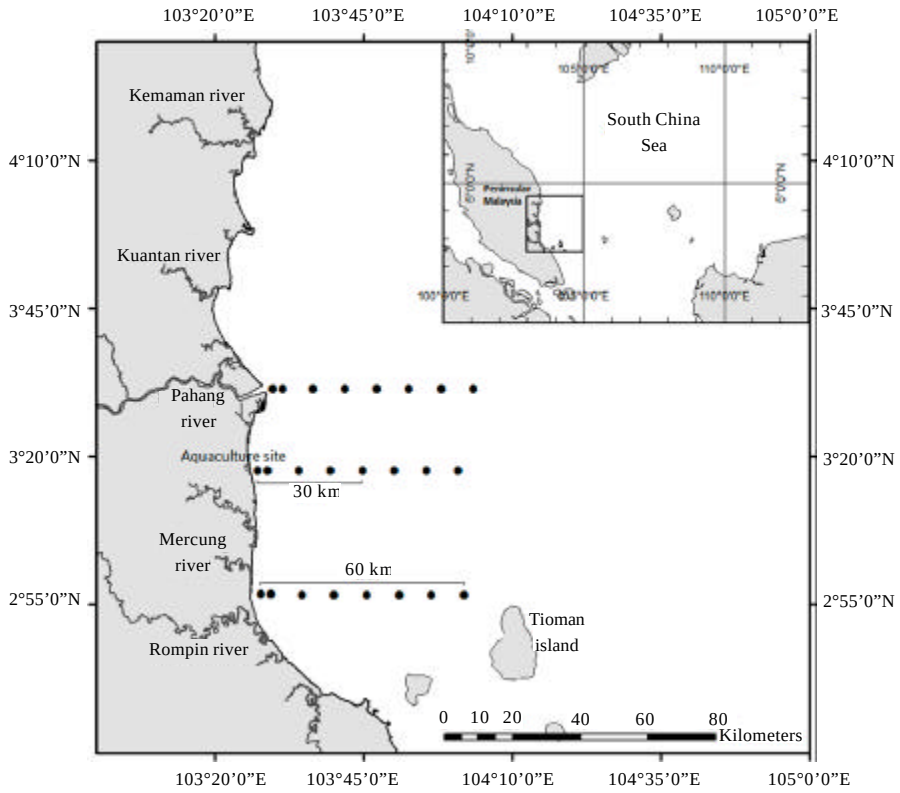

Fig. 1: The coastal region of Pahang, Malaysia showing several river systems which flow into the South China Sea and the location of the aquaculture sites. The dotted line indicates the location where the spectral signature of nLw 551 and Chl-a concentration were extracted (over 60 km from the coast)

MATERIALS AND METHODS

Satellite remote sensing data: In this study, five years of Aqua MODIS satellite images of normalized water-leaving radiance (nLw) and Sea Surface Temperature (SST) were downloaded from the NASAs GSFCs Distributed Active Archive Center (DAAC). Daily level 1 products with 1 km^2 spatial resolution at nadir, intersecting the region between 0.0°N to 10.0°N and from 100.0°E until 120.0°E were downloaded from the period of January 2006 to December 2010. Data were then processed using the SeaWiFS Data Analysis System (SeaDAS) software version 6.2 (O'Reilly *et al*., 1998; Chavula *et al*., 2009). Generated Level 3 products were subset from the images to geographic extents of 2.5°N to 4.5°N and 103.0°E to 104.45°E. Monthly composite data were then produced.

Image classification: Coastal water has different spectral reflectance due to its compositions. These characteristics observed from remotely sensed images were used to classify the area. Classified images were analyzed to understand the seasonal and interannual variability of the coastal waters off the East Coast of Peninsular Malaysia. Classification of this study was based on three channels of normalized water-leaving radiance. Training classes (Table 1) were applied to the images to define the classification region which has been adapted from the method of Thomas and

Table 1: Training classes used to define the classification regions

Water class	Training criteria	Classification characteristics
Class 1	High concentration of substances water region	Water region influenced by land with high concentration of suspended matter and has high reflectance value
Class 2	Coastal water	Spreading zone of high concentration water region
Class 3	Inner shelf water	Area near the coast as an intermediate between coastal water and off shore water
Class 4	Shelf water	Water areas that is not obviously associated with coastal water
Class 5	Off shore water	Region(s) of low reflectance value in all bands

Weatherbee (2006). Using the false color composites (nLw 412 (blue)/nLw 443 (green)/nLw 551 (red)) as a guide, five spectrally different classes were observed based on its characteristics. This technique provides a better visual guide of optical boundaries and regions of image product. Classification was then applied to the climatology composite images of MODIS (nLw (412), nLw (443) and nLw (551)) to simplify the seasonal differences according to spatial and temporal variations of surface water.

Empirical orthogonal function (EOF): Empirical Orthogonal Function (EOF) analysis was applied to the time series of the monthly averaged nLw 551 images. This method extracts the datasets into a series of orthogonal functions that describes the spatial and temporal variability within this study region (Baldacci *et al*., 2001; Mustapha *et al*., 2011). The dataset is presented by a few spatial modes with a total variance which explains the variability in a series of time.

Monthly composite images were standardized with the time-series and decomposed using the method of Polovina and Howell (2005):

$$F(x, t) = \sum_{i=1}^{N} a_i(t)c_i(x) \quad (1)$$

where, $a_i(t)$ are the principal component time-series or the expansion coefficients of the spatial components $c_i(x)$. The temporal and spatial components are calculated from the eigen vectors and eigen functions of the covariance matrix R, where $R=F' \cdot F$. This analysis results in N statistical modes, each with a vector of expansion coefficients related to the original data time-series by $a_i = Fc_i$ and a corresponding spatial component map c_i.

EOF gives the best result when applied to a series of no missing data (Ma *et al*., 2011). Interpolation was conducted to the images with missing data using the Distance Weighting function, which uses a set of reference data points that are weighted by a value corresponding with the distance between each point and the pixel to measure a pixel value inside the AOI. Maps were reconstructed using the basic monthly 1×1 km of the nLw 551 products.

Surface wind and current data: Wind data were downloaded from the Southeast Fisheries Science Center, NOAA Fisheries Service Environmental Research. The zonal and meridional ArcView gridded wind speed data were processed to get the magnitude and direction of the sea wind stress patterns of the region. These components were recalculated using the equation of wind stress, τ (kg m^{-1} s^{-2}) (Nezlin and DiGiacomo, 2005):

$$\tau = C_d \rho_{air} U^2$$

where, C_D is dimensionless drag coefficient (0.0013), ρ_{air} is air density (1.22 kg m^{-3}) and U is wind speed at 10 m above surface. The wind stress images were mapped using ArcGIS.

Surface current were obtained from the NOAA Ocean Surface Current Analysis (OSCAR) (Bonjean and Lagerloef, 2002). The monthly zonal and meridional datasets with 1 degree spatial and temporal resolution were downloaded for the 5 year period from January 2006 to December 2010. Current vector and magnitude were displayed and plotted using the Grid Analysis and Display System (GrADS).

RESULTS

Seasonal classification: Climatological classification of three visible channels of nLw (412/443/551) reveals five spectrally different classes for January 2006 until December 2010 (Fig. 2). The spatial distribution of the water classes depicted the optical evidence of summer and winter monsoon in this area. Each class represents a possible optical surface water property in the coastal region: Class 1 (high concentration of substances water region), Class 2 (coastal water),

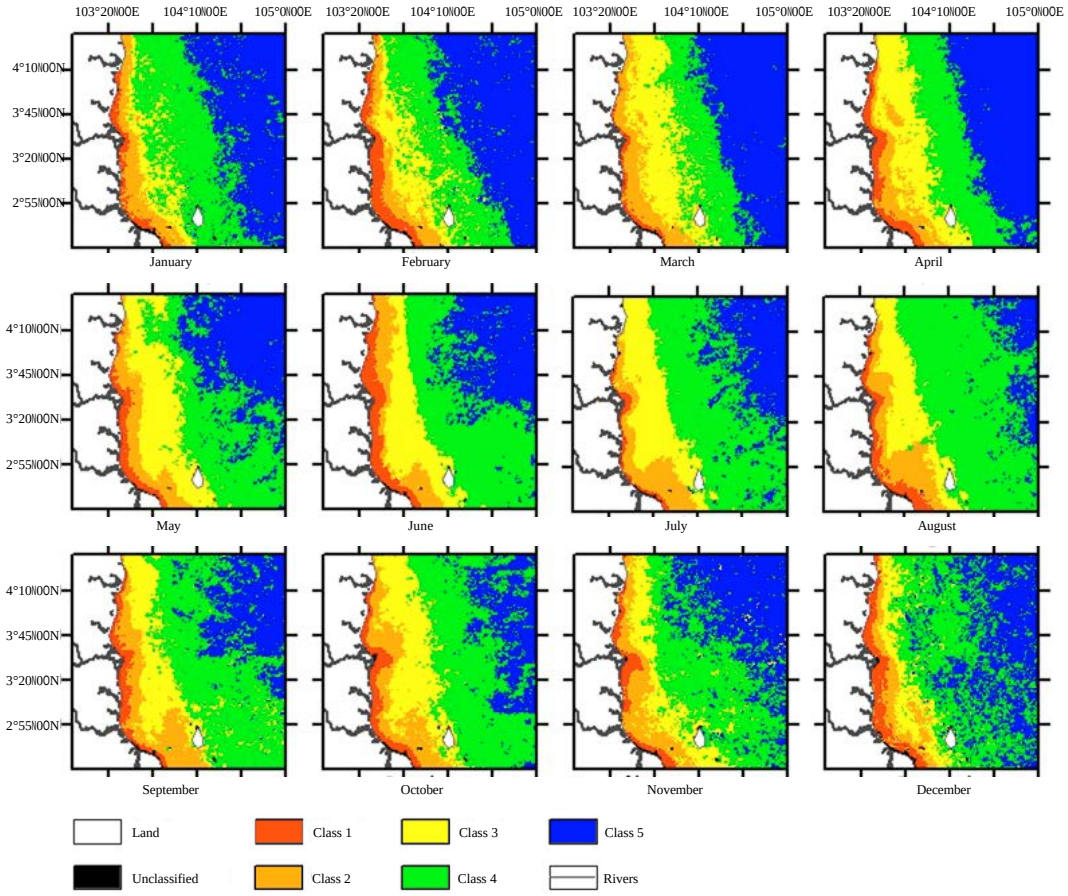

Fig. 2: Climatological classification of Malaysian Pahang coastal water. Five spectrally defined classes were present indicating the surface water optical characteristics. The classification series shows Class 1 (high concentration of substances water region), Class 2 (coastal water), Class 3 (inner shelf water), Class 4 (shelf water) and Class 5 (off shore water)

Class 3 (inner shelf water), Class 4 (shelf water) and Class 5 (offshore water). Class 1 is characterized as a water region influenced by land with high concentration of suspended matter. Class 1 and Class 2 occurred along the coastline. Class 3 and Class 4 indicated seasonal variations. Meanwhile, Class 5 water was distinctly identified as a region of low reflectance value and much further from the coastline.

Analyzing the occurrences of the spatial distributions of the five surface water classes of the climatology classification shows a strong seasonal variability in monthly timescales. During the northeast monsoon from November to March, Class 1 and Class 2 were observed to occupy the area along the coast. Class 3 occurred near the coast and Class 4 indicated the dispersion of coastal water toward the coastal direction. These classes were affected by wind forcing condition with a southward current movement. Meanwhile, Class 5 water was distinctly further from the coastline. Strong wind stress at 0.01-0.08 kg m^{-1} s^{-2} and surface current flow to the southwest direction with low sea surface temperature (25-30°C) indicated the northeast monsoon. Class position was clearly seen to be affected and being pushed to the northeast direction. The southwest monsoon occurred from May until September indicated by low wind stress with a value of 0.003-0.01 kg m^{-1} s^{-2}. Surface current propagated northeast and high sea surface temperature (28-35°C) occupied this region with Class 1 distributed along the coastline. Class 2 and Class 3 dispersion became wider due to the southwesterly wind. Class 4 mixed with Class 5 and spread offshore in pursuance of the wind direction.

The total area of each water classes and position indicated the influence of winter and summer monsoons on the surface water (Fig. 3). In the climatology data series, Class 1 covered a small area with the smallest value at 719 km^2 in July. Class 3 and Class 4 water showed an increase of spatial area during the southwest monsoon. Class 3 increased from March and remained until October and then started to decline in the area during the northeast monsoon. Class 4 started to increase from April to August with the maximum value at 21,649 km^2 in August and then declined. The total areas of Class 1 and Class 2 were not obviously different from the southwest to the northeast monsoons period; however, Class 2 water showed a position up to 75 km from the coast during the southwest monsoons indicating the spreading of the coastal waters due to the wind forcing condition.

Interannual variability of Pahang coastal surface water: Interannual variability of the Pahang coastal surface water was summarized by the EOF analysis of nLw 551. The EOF decomposition of the time series of monthly average MODIS images over the 5 year period indicated a total variance of 87.42% demonstrated in the first four modes (Fig. 4). The first mode of the EOF

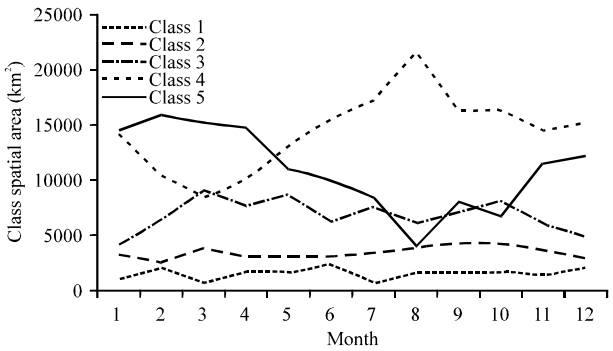

Fig. 3: Spatial area of classes from the classification of the monthly climatology

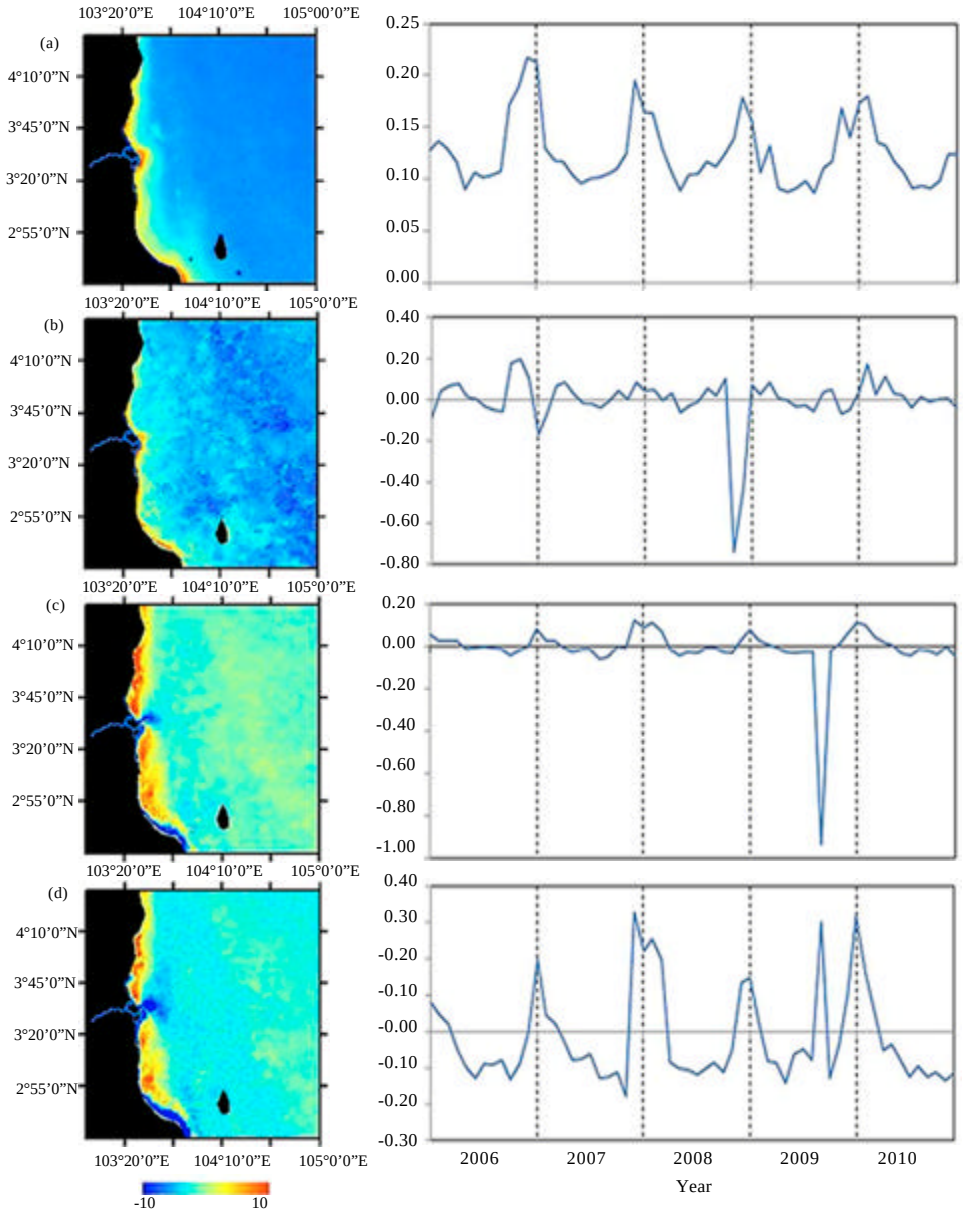

Fig. 4(a-d): EOF analysis showing the inter-annual variability of nLw 551 of the coastal water off Pahang. Each mode consists of spatial pattern (left) and the time-series (right), (a) The first mode represents 77.38% of the variance indicating the seasonal cycle, (b) The second mode represents 4.96% of the variance explaining the inter-monsoon period, (c) The third mode represents 3.17% of the variance explaining the Northeast monsoon and (d) The fourth mode represents 1.91% of the variance indicating the Southwest monsoon

analysis explained 77.38% of the variance (Fig. 4a). The time series indicated the seasonal cycle with high variability during the northeast and southwest monsoons. The spatial pattern showed positive signal detected along the coastline explaining the high variability of suspended matter.

High positive signals were detected in November to March each year and low negative signals were detected in May until September. This explained the variation during the winter and summer monsoon periods which occurred in this region.

The second mode of EOF explained 4.96% of the variance (Fig. 4b). The temporal pattern indicated the inter-monsoon period with high variability concentrated along the coastline mainly in April of each year. High positive signals were also detected during October in 2006, 2007, 2008 and 2009. Negative signals were detected offshore. This explained the variation caused by the occurrences of wind and current changing direction between the two periods of the northeast and southwest monsoon in this area.

The third EOF mode explained 3.17% of the total variance indicating the northeast monsoon (Fig. 4c). Positive signals were detected toward the coastline associated with river discharge and strong wind during this period. Its temporal signature indicated high positive signals in January 2006, December 2007, January 2009 and February 2010. Meanwhile, mode 4 explained the variability during the southwest monsoon period with 1.91% of the total variance (Fig. 4d). Variability was observed at the mouth of the Pahang River and the coastal water region which was detected by the negative signals. Surface pattern that spread further from the coast was observed.

Distribution of suspended particle and Chl-a: Using the monthly composite of nLw 551, the coastal water was analyzed to determine suspended matter distribution in the along-shelf direction. Analyzing the spatial data from the mouth of the Pahang River (dominant river system), the Mercung River (smaller river system) and the aquaculture site (up to 60 km offshore) indicated high variability which was significantly correlated with surface Chl-a distribution.

It was observed that near the coast during the northeast monsoon, nLw 551 values of Pahang River, Mercung River and the aquaculture area were detected to be above 1.5 mW cm^{-2} μm^{-1} sr^{-1}. However, Chl-a was detected to be slightly higher than nLw 551 at those three profiles. Mercung River recorded higher values of nLw 551 and Chl-a in comparison to Pahang River and the aquaculture area. The values of nLw 551 and Chl-a were highest 5 km from the coast with 4.05 mW cm^{-2} μm^{-1} s^{-1} and 5.71 mg m^{-3}, respectively. Further away from the coast at about 5 km and above, the values started to decrease sharply at Pahang River and the aquaculture area and became constant at 30 km from the coast but decreased gradually for the Mercung River. The values were constant at a distance exceeding 30 km from the coast. It was observed that at 5 km away from the coast, all areas had values of nLw 551 higher than Chl-a. This can be observed from the monthly images of February 2010 representing the northeast monsoon (Fig. 5).

During the southwest monsoon, at the coast, nLw 551 was below 1.5 mW cm^{-2} μm^{-1} sr^{-1}. However, Chl-a was still higher than nLw 551. Mercung river still recorded higher values of nLw 551 and Chl-a compared to Pahang river and the aquaculture area. At Pahang river and the aquaculture area, Chl-a was high until 5 km from coast. The values decreased and became constant at a distance of more than 30 km from the coast off Pahang River and further than 20 km for Mercung River and the aquaculture area. From the coast to a distance of 20 km, Chl-a was observed higher than nLw 551 and further away, Chl-a was slightly below than the nLw 551 values. This pattern is represented by the August 2010 monthly images.

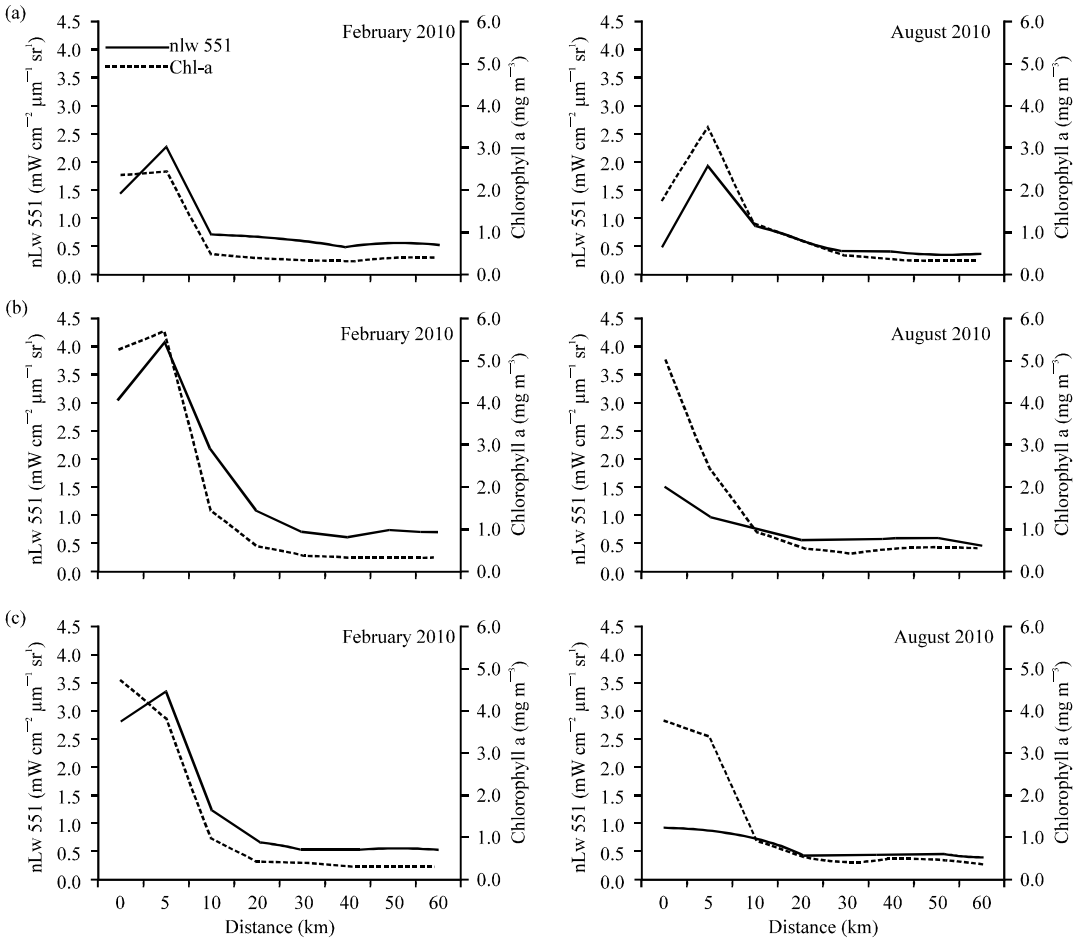

Fig. 5(a-c): nLw 551 spectral signature and Chl-a concentration over 60 km from the coast of (a) Pahang river, (b) Mercung river and (c) The aquaculture site in February 2010 representing the northeast monsoon and August 2010 for the southwest monsoon

DISCUSSION

Assessing and understanding the variability within this region is necessary to ensure sustainable management of coastal areas especially for fisheries practices. The coastal region of Pahang is located in the South China Sea and therefore, the seasonal variability of the coastal water is governed by the winter and summer monsoons. Its circulation pattern also has a distinct seasonal behavior (Jilan, 2004); hence, the properties of water can be defined by its differences in spectral signature. Multispectral classification shows variability in each class based on the optical properties of the near surface water. The Pahang coastal water is highly influenced by the monsoon period over the South China Sea (Chang *et al*., 2006; Wang *et al*., 2009; Kueh and Lin, 2010). Mode 1 of the EOF analysis suggested that seasonal variability occurs each year indicating low and high signals that represent the wet and dry monsoon period. Meanwhile, the inter-monsoon period as indicated by mode 2 of the EOF analysis shows the onset of summer and winter monsoons affecting this region. Negative signals were detected offshore while positive signals occupied the area along the coast and spread toward the offshore direction. This occurrence shows the movements of surface water due to the changing of wind direction. Many studies have also shown

that the seasonal progression in this region is highly influenced by wind propagation and current. Wind forcing condition brings the circulation of low and high SST to the South China Sea region (Wang *et al*., 2009).

According to Kueh and Lin (2010), the transition and onset of these monsoon periods happens due to atmospheric internal dynamics, intra-seasonal oscillation and sea/land surface conditions. The evidence of the northeast and southwest monsoon influencing the coastal area was explained by the propagation of wind and current movement of the South China Sea (Fig. 6). The response of the coastal water to these occasions is significant. During the northeast monsoon, Class 2, Class 3 and Class 4 are pushed to the coast in pursuance of the wind and current direction. In December 2009, the southwestward propagation of wind stress moved the surface current to the coastal direction and brought low SST to this region (Fig. 6a). Meanwhile, the Inter-monsoon April marks the end of the northeast winter monsoon. The southwest summer monsoon appears in this region in May and continues until September. Seasonal progression of Class 2, Class 3 and Class 4 shows a spreading pattern to the northeast and offshore direction according to the wind and current movement. High sea surface temperature that happens in this region occurs with the movements of the surface water in accordance with the northeasterly wind stress (Fig. 6b).

The variability of coastal water is also highly significant due to the dynamic outflow of freshwater which carries loads of sediments, organic material and dissolved substances into the ocean. The description of water characteristics in this area can be defined optically through a series of classified water bodies. The spectral signature indicated high value of Class 1 (high concentration of substances water region) which extends further offshore along the coastline. The property of this area is governed by wind effect and rainfall that occurs along the east coast of Peninsular Malaysia during winter (Wang *et al*., 2009). It is suggested that the strong northeast wind will spread the suspended materials and cause mixing in the water column. Class 1 water is also influenced by relative changes in discharged water by rivers. High concentration of suspended material increases water turbidity and gives an apparent pattern to its spectral signature. However, from May until September, river discharge and wind magnitude are relatively weak and the surface water is confined to the coastal area. This variability was also explained by the EOF analysis of MODIS nLw 551 monthly composite images. The temporal and spatial variation of nLw 551 distribution over the 5 year period revealed the influence of seasonal effect of wind and river discharge. Optical properties of nLw 551 distribution are well suited for quantifying the relative deposition and suspended matter composition that indicates important interannual changes. It has been shown that high distribution of this suspended matter influences the surrounding waters by increasing its turbidity and limiting the chlorophyll concentration (Radiarta and Saitoh, 2008). During the wet season, large amounts of suspended matter are discharged by rivers due to high rainfalls that occur within the terrestrial environments (Ni *et al*., 2008; Pietrzak *et al*., 2011).

The spatial signature showed high variability near the coast indicating high concentration of suspended matter along the coastline especially from November until March each year. This study revealed that the coastal surface water was influenced by wind stress. It followed the movement of wind direction as a result of Ekman transport (Walker *et al*., 2005). Mode 3 of the EOF analysis indicated re-suspension of deposited sediments and suspended materials. Discharged water from rivers around the area also contributes to the high concentration of suspended matter as a result of strong wind. River discharges and the aquaculture site within the area have significant effects on the coastal surface signature value with seasonal differences. High rainfall during the months of November and December in this region results in high suspended matter and nutrient

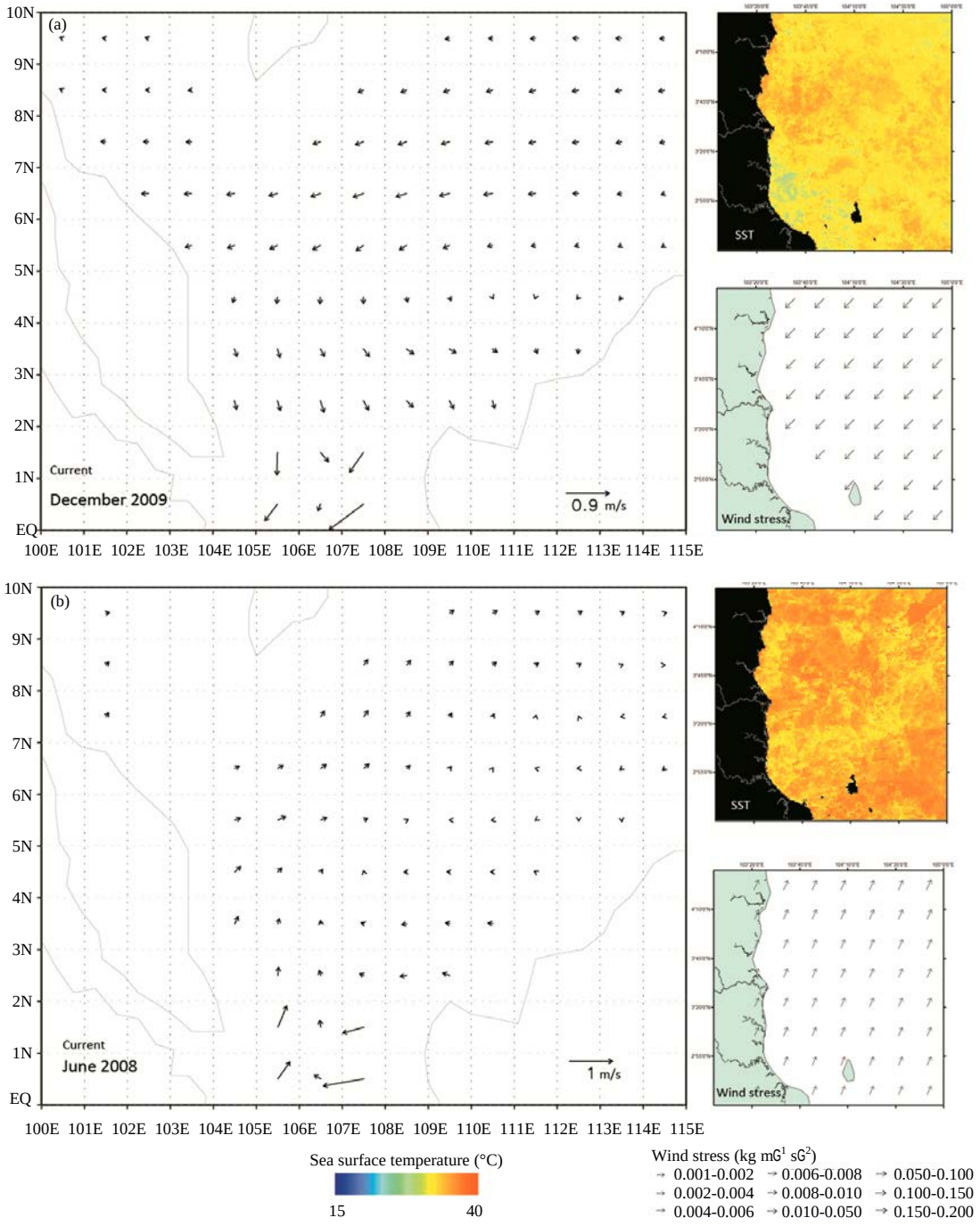

Fig. 6(a-b): Current profile in the South China Sea (left panel), SST (upper right panel) and wind stress vector and magnitude (lower right panel), (a) December 2009 representing the Northeast monsoon and (b) June 2008 representing the Southwest monsoon. The Northeast monsoon indicatesthe southwest propagation of wind stress and surface current which brings low SST to this region, while during the Southwest monsoon, high SST occurs along with the movement of the surface water in accordance with the northeasterly wind stress

composition during the Northeast monsoon due to the terrestrial discharge along the coastline (Penaflor *et al*., 2007; Wang *et al*., 2009). Inputs of nutrients in coastal water have been reported to increase chlorophyll concentration (Kasai *et al*., 1997; Paez-Osuna *et al*., 1998; Penaflor *et al*., 2007; Dasgupta *et al*., 2009). However, the presence of high suspended matter especially sediment or CDOM can cause a limitation of Chl-a detection in surface water (Zimba and Gitelson, 2006; Gitelson *et al*., 2007; Radiarta and Saitoh, 2008; Reifel *et al*., 2009).

Meanwhile, during the southwest monsoon, the lower river discharge results in lower surface signature as detected by Mode 4 of the EOF analysis. Variability of nLw 551 constituents provides information on the dynamic distribution and concentration of Chl-a in the environment (Gitelson *et al*., 2007). Study has shown that water mixing and river discharge show high chlorophyll value nearer to the coast compared to deeper waters (Dasgupta *et al*., 2009). This can be observed at the mouth of Pahang and Mercung River where lower Chl-a concentration near the coast occurs due to higher concentration of suspended matter during the Northeast monsoon. However, river discharges and wind forcing condition during the southwest monsoon lead to higher concentration of Chl-a within the coastal region due to lower occurrences of suspended matter.

CONCLUSION

Interannual and seasonal variability of the coastal water off Pahang was described by the classification approach that separates the surface water into five spectral classes based on its optical characteristics: high concentration of substances water region, coastal water, inner shelf water, shelf water and offshore water. The variability indicates the influence of terrestrial outflow, wind and current propagation in this area indicating the occurrences of the northeast and southwest monsoon. High variability along the coastal area during the northeast monsoon is related to the strong wind patterns and the lower variability during the southwest monsoon is a result of weakened wind. Hence, understanding the dynamic processes within this region is greatly important. This contributes to an integrated coastal management and planning that could provide benefits to the coastal area as well as the productivity of this region.

ACKNOWLEDGMENTS

The authors would like to thank the NASA Goddard Space Flight Center for the MODIS-Aqua Level 1A data, the Environmental Research Division (ERD) Live Access Server for the wind data and also NOAA Ocean Surface Current Analysis (OSCAR) for the current data used in this study. This work has been supported by the UKM University-Industry Grant (Industri-2011-012), the Ministry of Higher Education Fundamental Research Grant Scheme (FRGS/1/2012/STWN)S/UKM/02/3) and The Long Team Research Grant Scheme LRGS-LRGS-TD/2011/UKM/PG/01 and the Ministry of Science, Technology and Innovation Science Fund (04-01-02-SF0589). We would also like to thank the anonymous reviewers for their very helpful comments.

REFERENCES

Baldacci, A., G. Corsini, R. Grasso, G. Manzella and J.T. Allen *et al*., 2001. A study of the Alboran sea mesoscale system by means of empirical orthogonal function decomposition of satellite data. J. Mar. Syst., 29: 293-311.

Bonjean, F. and G.S.E. Lagerloef, 2002. Diagnostic model and analysis of the surface currents in the tropical pacific ocean. J. Phys. Oceanogr., 32: 2938-2954.

Chang, C.P., Z. Wang and H. Hendon, 2006. The Asian Winter Monsoon. In: The Asian Monsoon, Wang, B. (Ed.). Chapter 3. Springer, Chichester, UK., ISBN-13: 9783540377221, pp: 88-128.

Chavula, G., P. Brezonik, P. Thenkabail, T. Johnson and M. Bauer, 2009. Estimating chlorophyll concentration in Lake Malawi from MODIS satellite imagery. Phys. Chem. Earth, 34: 755-760.

Darecki, M. and D. Stramski, 2004. An evaluation of MODIS and SeaWiFS bio-optical algorithms in the Baltic Sea. Remote Sens. Environ., 89: 326-350.

Dasgupta, S., R.P. Singh and M. Kafatos, 2009. Comparison of global chlorophyll concentrations using MODIS data. Adv. Space Res., 43: 1090-1100.

Gitelson, A.A. J.F. Schalles and C.M. Hladik, 2007. Remote chlorophyll: A retrieval in turbid, productive estuaries: Chesapeake Bay case study. Remote Sens. Environ., 109: 464-472.

Jilan, S., 2004. Overview of the South China Sea circulation and its influence on the coastal physical oceanography outside the Pearl River Estuary. Cont. Shelf Res., 24: 1745-1760.

Kasai, H., H. Saito, A. Yoshimori and S. Taguchi, 1997. Variability in timing and magnitude of spring bloom in the Oyashio region, the Western subartic Pacific off Hokaido, Japan. Fish. Oceanogr., 6: 118-129.

Kueh, M.T. and S.C. Lin, 2010. A climatological study on the role of the South China Sea monsoon onset in the development of the East Asian summer monsoon. Theor. Applied Climatol., 99: 163-186.

Li, J., S. Gao and Y. Wang, 2010. Delineating suspended sediment concentration patterns in surface waters of the Changjiang Estuary by remote sensing analysis. Acta Oceanol. Sin., 29: 38-47.

Lihan, T., S.I. Saitoh, T. Iida, T. Hirawake and K. Iida, 2008. Satellite-measured temporal and spatial variability of the Tokachi River plume. Estuarine Coastal Shelf Sci., 78: 237-249.

Ma, J., H. Zhan and Y. Du, 2011. Seasonal and interannual variability of surface CDOM in the South China sea associated with El Nino. J. Mar. Syst., 85: 86-95.

Mustapha, A.M., T. Lihan and S. Saitoh, 2011. Determination of physical processes influencing Chl a distribution using remotely sensed images. Pak. J. Biol. Sci., 14: 82-90.

Nezlin, N.P. and P.M. DiGiacomo, 2005. Satellite ocean color observations of stormwater runoff plumes along the San Pedro Shelf (Southern California) during 1997-2003. Continental Shelf Res., 25: 1692-1711.

Nezlin, N.P., P.M. DiGiacomo, D.W. Diehl, B.H. Jones and S.C. Johnson *et al*., 2008. Stormwater plume detection by MODIS imagery in the Southern California coastal ocean. Estuar. Coast. Shelf Sci., 80: 141-152.

Ni, H.G., F.H. Lu, X.L. Luo, H.Y. Tian and E.Y. Zeng, 2008. Riverine inputs of total organic carbon and suspended particulate matter from the Pearl River Delta to the coastal ocean off South China. Mar. Pollut. Bull., 56: 1150-1157.

O'Reilly, J.E., S. Maritorena, B.G. Mitchell, D.A. Siegel and K.L. Carder *et al*., 1998. Ocean color chlorophyll algorithms for seaWiFS. J. Geophys. Res., 103: 24937-24953.

Paez-Osuna, F., S.R. Guerrero-Galvan and A.C. Ruiz-Fernandez, 1998. The environmental impact of shrimp aquaculture and the coastal pollution in Mexico. Mar. Pollut. Bull., 36: 65-75.

Penaflor, E.L., C.L. Villanoy, C.T. Liu and L.T. David, 2007. Detection of monsoonal phytoplankton blooms in Luzon Strait with MODIS data. Remote Sens. Environ., 109: 443-450.

Pietrzak, J.D., G.J. de Boer and M.A. Eleveld, 2011. Mechanisms controlling the intra-annual mesoscale variability of SST and SPM in the Southern North Sea. Cont. Shelf Res., 31: 594-610.

Polovina, J.J. and E.A. Howell, 2005. Ecosystem indicators derived from satellite remotely sensed oceanographic data for the North Pacific. ICES J. Mar. Sci., 62: 319-327.

Radiarta, I.N. and S.I. Saitoh, 2008. Satellite-derived measurements of spatial and temporal chlorophyll-a variability in Funka Bay, Southwestern Hokkaido, Japan. Estuarine Coastal Shelf Sci., 79: 400-408.

Reifel, K.M., S.C. Johnson, P.M. DiGiacomo, M.J. Mengel, N.P. Nezlin, J.A. Warrick and B.H. Jones, 2009. Impacts of stormwater runoff in the Southern California Bight: Relationships among plume constituents. Cont. Shelf Res., 29: 1821-1835.

Sasmal, S.K., 1997. Optical classification of waters in the Eastern Arabian Sea. J. Indian Soc. Remote Sens., 25: 73-78.

Schalles, J.F., 2006. Optical Remote Sensing Techniques to Estimate Phytoplankton Chlorophyll a Concentrations in Coastal Waters with Varying Suspended Matter and CDOM Concentrations. In: Remote Sensing of Aquatic Coastal Ecosystem Processes: Science and Management Applications, Richardson, L. and E. Ledrew (Eds.). Springer, Dordrecht, Netherlands, pp: 27-79.

Schroeder, T., M.J. Devlin, V.E. Brando, A.G. Dekker, J.E. Brodie, L.A. Clementson and L. McKinna, 2012. Inter-annual variability of wet season freshwater plume extent into the Great Barrier Reef lagoon based on satellite coastal ocean colour observations. Mar. Pollut. Bull., 65: 210-223.

Thomas, A.C. and R.A. Weatherbee, 2006. Satellite-measured temporal variability of the Columbia River plume. Remote Sensing Environ., 100: 167-178.

Tiwari, S.P. and P. Shanmugam, 2011. An optical model for the remote sensing of coloured dissolved organic matter in coastal/ocean waters. Estuarine Coastal Shelf Sci., 93: 396-402.

Walker, N.D., W.J. Jr. Wiseman L.J. Jr. Rouse and A. Babin, 2005. Effects of river discharge, wind stress and slope eddies on circulation and the satellite-observed structure of the Mississippi River plume. J. Coastal. Res., 21: 1228-1244.

Wang, B., L. Ho, Y. Zhang and M.M. Lu, 2004. Definition of South China Sea monsoon onset and commencement of the East Asia summer monsoon. J. Clim., 17: 699-710.

Wang, B., F. Huang, Z. Wu, J. Yang, X. Fu and K. Kikuchi, 2009. Multi-scale climate variability of the South China Sea monsoon: A review. Dyn. Atmos. Oceans, 47: 15-37.

Wang, M., W. Shi and J. Tang, 2011. Water property monitoring and assessment for China's inland Lake Taihu from MODIS-aqua measurements. Remote Sens. Environ., 115: 841-854.

Yuan, D., J. Zhu, C. Li and D. Hu, 2008. Cross-shelf circulation in the Yellow and East China Seas indicated by MODIS satellite observations. J. Mar. Syst., 70: 134-149.

Zhang, M.R., L.O. Hall, D.B. Goldgof and F.E. Muller-Karger, 2000. Knowledge-guided classification of coastal zone color images off the West Florida shelf. Int. J. Pattern Recognit. Artif. Intell., 14: 987-1007.

Zimba, P.V. and A. Gitelson, 2006. Remote estimation of chlorophyll concentration in hyper-eutrophic aquatic systems: Model tuning and accuracy optimization. Aquaculture, 256: 272-286.